

KNOWLEDGE MODELS OF PHOTOBIOREACTORS AND THEIR PATH-INTEGRAL FORMULATION

Jérémi DAUCHET, Jean-François CORNET, C.-Gilles DUSSAP,
Guillaume FOIN, Fabrice GROS, Céline LAROCHE, Laurent POUGHON,
Thomas VOURC'H, Daniel YAACOUB



MELISSA conference, 8-10/11 2022

Institut Pascal

GEPEB : génie des procédés, énergétique et biosystèmes



INSTITUT
PASCAL

Sciences de l'ingénierie et des systèmes

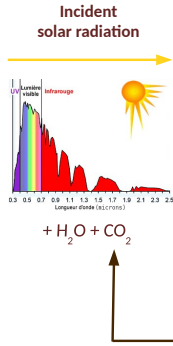
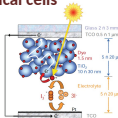
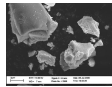


Photo-reactive Systems Engineering research group

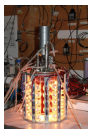
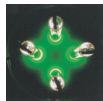
Photo-electrochemical cells



Photoreactors



Photobioreactors

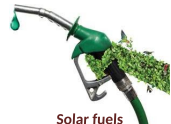


Artificial photosynthesis

Hydrogen, syngaz,
methanol...

Biofuel,

Raw molecules for chemistry,
high valuable products



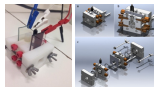
Biomass converted
In bio-refinery



Natural
photosynthesis

O_2, \dots
closed-loop ecosystems

Methodology



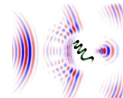
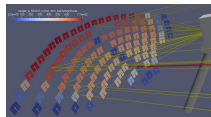
Photoelectrochemical cell



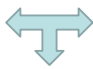
Photoreactor



Photobioreactor



High accuracy benches designed for
model validation at the lab scale



Development of knowledge models

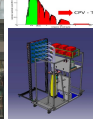
Design of innovative demonstrators with high energy and kinetic efficiencies
(model-based optimization)

Dilution



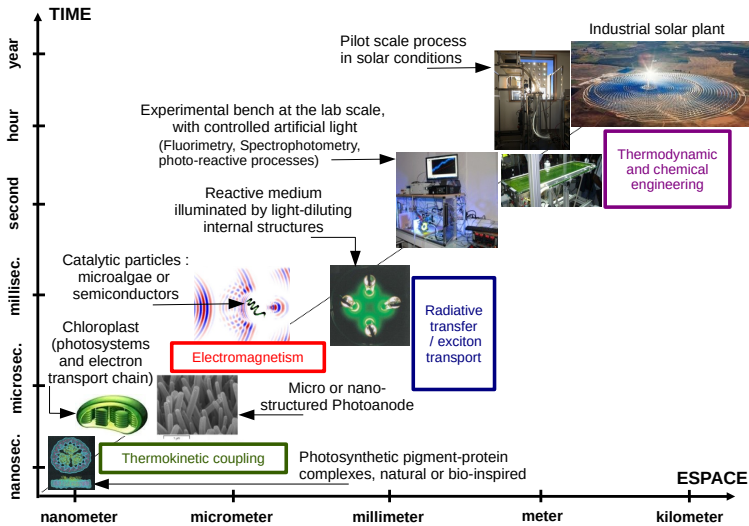
DiCoFluV - solar dilution photoreactor
(30 L - 1 m² - héliostat 2 m²)

Hybridization

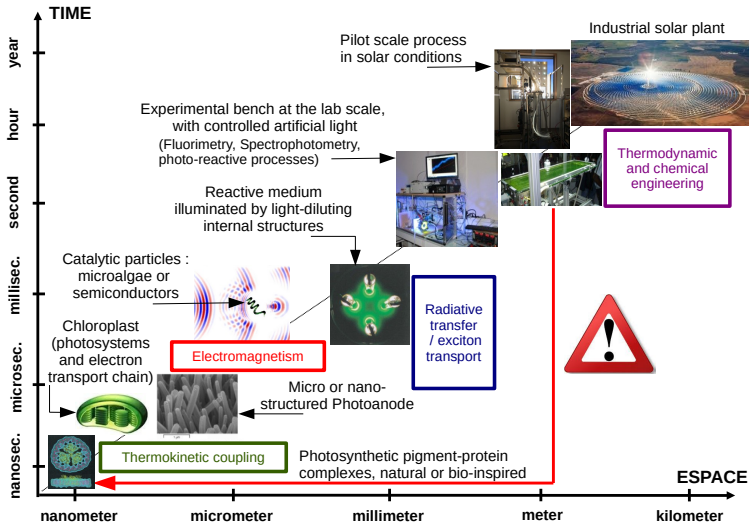


DiCoFluV-Hy - hybrid solar reactor
(2 L - 0,03 m² - héliostat 0,1 m²)

Phenomenological, geometric and temporal complexity

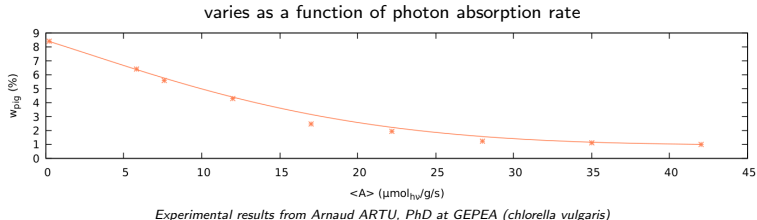


Feedback loop on radiative properties



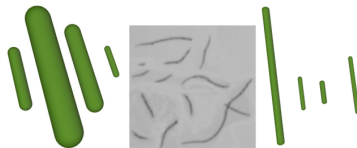
Feedback loop on radiative properties

- via pigment content



- via micro-organism geometry

shape and size distribution vary as a function of mixing



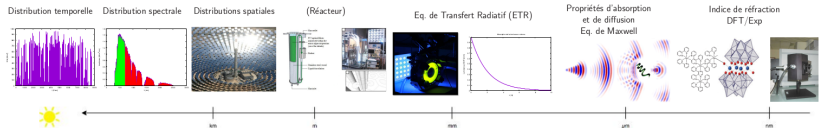
Size distribution,
fixed average aspect ratio

Optical microscopy

size and aspect ratio
distribution

Experimental results from Vincent Rochat, PhD at Institut Pascal (*Arthrosphaera platensis*)

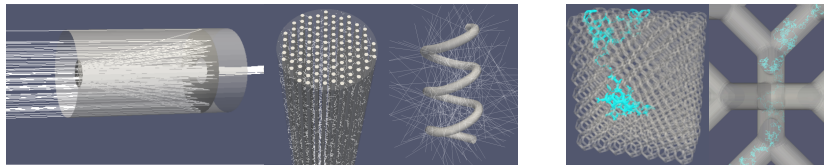
Extending Feynmann-Kac path integral formulation



$$\langle \bar{r}_{O_2} \rangle = \phi \int_{\Delta t} DNI(t) dt \int_{\Delta \nu} p_\nu(\nu) d\nu \int_V \frac{1}{V} dr r O_2 \left(r, \int_{D_\Gamma} p_\Gamma(\gamma) d\gamma k_{a,\nu} e^{-C \int_G p_G(g) dg \sigma_{a,\nu} (\sum_n k_{s,n,\nu}) I(\gamma)} \right)$$

Renewed interpretation of the process:

- ① highlighting the scales, phenomenon and their hierarchical coupling
- ② bringing random walks that propagate in a multi-physics multi-scales path-space



A research topic in the french consortium EDStar (www.edstar.cnrs.fr/prod/fr/):
recent advances to handle couplings, including nonlinearities

Monte Carlo method

Numerical simulations benefit from path-integral formulations:

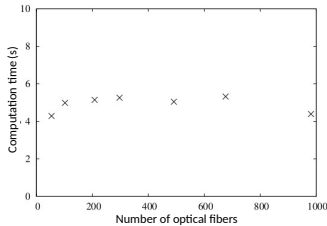
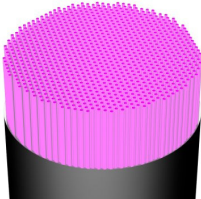
- convergence rates is independent of the number of nested integrals
→ *phenomenological complexity*

	C_x (kg m^{-3})		$\tilde{\sigma}_\nu(d_m)$	$\sigma_{a,\nu}$	$L_\nu(\vec{x}, \vec{u}, t)$	$\mathcal{A}(\vec{x}, t)$	$r_x(\vec{x}, t)$	$\langle r_x(t) \rangle$	$\langle \bar{r}_x \rangle$
<i>Arthrosphaera platensis</i>	1	t_{brut} (s)	1.096	1.339	6.39	11.11	96.4	64.8	80.6
		ϵ (%)	0.0505	0.0813	0.0988	0.213	0.0212	0.0178	0.0915
		$t_{1\%}$ (s)	0.00280	0.00885	0.06228	0.502	0.043	0.0205	0.674
	4	t_{brut} (s)			18.03	17.37	2383	963	950
		ϵ (%)			0.402	0.958	0.145	0.076	0.154
		$t_{1\%}$ (s)			2.91	15.93	49.9	5.59	22.21

Monte Carlo method

Numerical simulations benefit from path-integral formulations:

- convergence rates is independent of the number of nested integrals
→ *phenomenological complexity*
- computer graphics tools for orthogonal handling of the geometric data
→ *fast path-tracing insensitive to geometric complexity*



Monte Carlo method

Numerical simulations benefit from path-integral formulations:

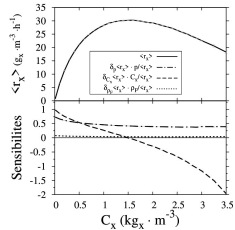
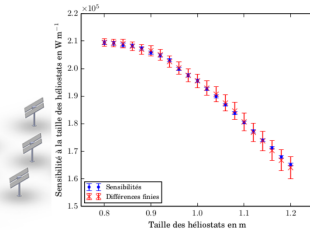
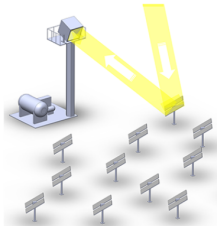
- convergence rates is independent of the number of nested integrals
→ *phenomenological complexity*
- computer graphics tools for orthogonal handling of the geometric data
→ *fast path-tracing insensitive to geometric complexity*
→ *inverse design*



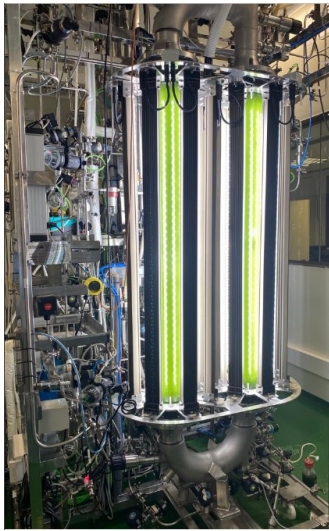
Monte Carlo method

Numerical simulations benefit from path-integral formulations:

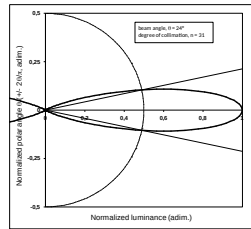
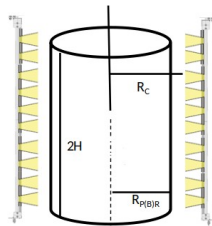
- convergence rates is independent of the number of nested integrals
→ *phenomenological complexity*
- computer graphics tools for orthogonal handling of the geometric data
→ *fast path-tracing insensitive to geometric complexity*
→ *inverse design*
- sensitivity analysis
→ *guides optimization*



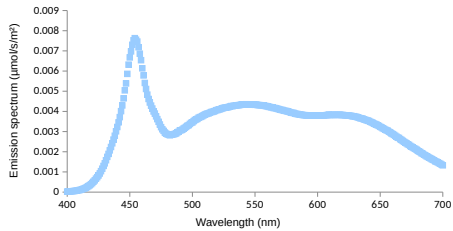
UAB photobioreactor configuration



Cylindrical photobioreactor



Radial illumination by 8 panels made of 80 white LEDs + optics $\theta = 24^\circ$



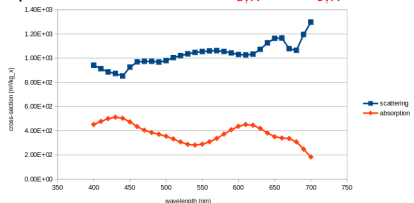
A focus on radiative transfer and thermokinetic coupling

- Radiative transfer equation

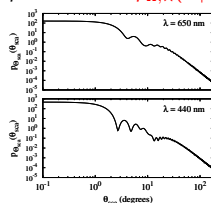
$$\omega \cdot \text{grad}_x L_\lambda(x, \omega) = -C_x (\sigma_{a,\lambda} + \sigma_{s,\lambda}) L_\nu(x, \omega) + C_x \sigma_{s,\lambda} \int_{4\pi} L_\lambda(x, \omega') p_{\Omega,\lambda}(\omega|\omega') d\omega'$$

- Radiative properties (schiff: www.meso-star.com/projects/schiff/schiff.html)

Arthrospira platensis: cross-sections $\sigma_{a,\lambda}$ and $\sigma_{s,\lambda}$



phase function $p_{\Omega,\lambda}(\omega|\omega')$



Hybrid model and experimental results from Vincent Rochat, PhD at Institut Pascal

- Thermokinetic coupling law at each point x

$$r_{O_2}(x) = Cx \Phi \rho_m \frac{K}{K + A(x)} A(x) \quad ; \quad A(x) = \sigma_{a,\lambda} \int_{4\pi} L_\lambda(x, \omega) d\omega$$

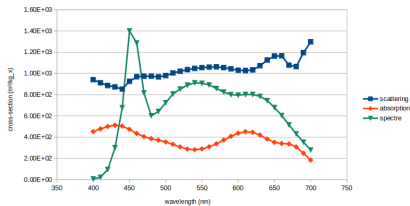
- Volume averages: $\langle A \rangle$ and $\langle r_{O_2} \rangle$

Two-flux approximation for radiative transfer

- Grey approximation

$$\bar{\sigma}_i = \int_{\lambda_{min}}^{\lambda_{max}} f_{source}(\lambda) \sigma_{i,\lambda} d\lambda$$

$$\bar{p}_{\Omega} = \int_{\lambda_{min}}^{\lambda_{max}} \frac{f_{source}(\lambda) \sigma_{s,\lambda}}{\bar{\sigma}_s} p_{\Omega,\lambda} d\lambda$$



- Two-flux approximation for 1d cylindrical systems

$$\mathcal{A}(x) = 2\bar{\sigma}_a q_0 \frac{\mathcal{I}_0(\delta r)}{\mathcal{I}_0(\delta R) + \alpha \mathcal{I}_1(\delta R)}$$

with \mathcal{I} the Bessel functions, q_0 the incident flux density,

$$\delta = C_x \sqrt{\bar{\sigma}_a (\bar{\sigma}_a + 2b\bar{\sigma}_s)}, \quad \alpha = \sqrt{\frac{\bar{\sigma}_a}{\bar{\sigma}_a + 2b\bar{\sigma}_s}}, \quad b = \int_{2\pi} - p_{\Omega,\lambda}(\omega|\omega') d\omega$$

Can be implemented in spreadsheets and programmable logic controllers

Results

$C_x = 0.05 \text{ g/l}$	Ref. (1% err.)	2-flux	diff.	max
$\langle \mathcal{A} \rangle (\mu\text{mol}/\text{s}/\text{m}^3)$	43550	34944	20%	46667
$\langle r_{O_2} \rangle (\text{mol}/\text{l}/\text{h})$	$4.39 \cdot 10^{-4}$	$4.35 \cdot 10^{-4}$	1%	$19 \cdot 10^{-4}$
$C_x = 0.10 \text{ g/l}$	Ref. (1% err.)	2-flux	diff.	max
$\langle \mathcal{A} \rangle (\mu\text{mol}/\text{s}/\text{m}^3)$	46200	42522	8%	46667
$\langle r_{O_2} \rangle (\text{mol}/\text{l}/\text{h})$	$8.45 \cdot 10^{-4}$	$8.30 \cdot 10^{-4}$	2%	$19 \cdot 10^{-4}$
$C_x = 0.20 \text{ g/l}$	Ref. (1% err.)	2-flux	diff.	max
$\langle \mathcal{A} \rangle (\mu\text{mol}/\text{s}/\text{m}^3)$	46450	42630	8%	46667
$\langle r_{O_2} \rangle (\text{mol}/\text{l}/\text{h})$	$13.9 \cdot 10^{-4}$	$13.6 \cdot 10^{-4}$	2%	$19 \cdot 10^{-4}$

Results

$C_x = 0.05 \text{ g/l}$	Ref. (1% err.)	2-flux	diff.	max
$\langle \mathcal{A} \rangle (\mu\text{mol}/\text{s}/\text{m}^3)$	43550	34944	20%	46667
$\langle r_{O_2} \rangle (\text{mol}/\text{l}/\text{h})$	$4.39 \cdot 10^{-4}$	$4.35 \cdot 10^{-4}$	1%	$19 \cdot 10^{-4}$
$C_x = 0.10 \text{ g/l}$	Ref. (1% err.)	2-flux	diff.	max
$\langle \mathcal{A} \rangle (\mu\text{mol}/\text{s}/\text{m}^3)$	46200	42522	8%	46667
$\langle r_{O_2} \rangle (\text{mol}/\text{l}/\text{h})$	$8.45 \cdot 10^{-4}$	$8.30 \cdot 10^{-4}$	2%	$19 \cdot 10^{-4}$
$C_x = 0.20 \text{ g/l}$	Ref. (1% err.)	2-flux	diff.	max
$\langle \mathcal{A} \rangle (\mu\text{mol}/\text{s}/\text{m}^3)$	46450	42630	8%	46667
$\langle r_{O_2} \rangle (\text{mol}/\text{l}/\text{h})$	$13.9 \cdot 10^{-4}$	$13.6 \cdot 10^{-4}$	2%	$19 \cdot 10^{-4}$

Results

$C_x = 0.05 \text{ g/l}$	Ref. (1% err.)	2-flux	diff.	max
$\langle \mathcal{A} \rangle (\mu\text{mol}/\text{s}/\text{m}^3)$	43550	34944	20%	46667
$\langle r_{O_2} \rangle (\text{mol}/\text{l}/\text{h})$	$4.39 \cdot 10^{-4}$	$4.35 \cdot 10^{-4}$	1%	$19 \cdot 10^{-4}$
$C_x = 0.10 \text{ g/l}$	Ref. (1% err.)	2-flux	diff.	max
$\langle \mathcal{A} \rangle (\mu\text{mol}/\text{s}/\text{m}^3)$	46200	42522	8%	46667
$\langle r_{O_2} \rangle (\text{mol}/\text{l}/\text{h})$	$8.45 \cdot 10^{-4}$	$8.30 \cdot 10^{-4}$	2%	$19 \cdot 10^{-4}$
$C_x = 0.20 \text{ g/l}$	Ref. (1% err.)	2-flux	diff.	max
$\langle \mathcal{A} \rangle (\mu\text{mol}/\text{s}/\text{m}^3)$	46450	42630	8%	46667
$\langle r_{O_2} \rangle (\text{mol}/\text{l}/\text{h})$	$13.9 \cdot 10^{-4}$	$13.6 \cdot 10^{-4}$	2%	$19 \cdot 10^{-4}$

Results

With radiative properties for *Arthrospira platensis* in different culture conditions
(reference model solved with Monte Carlo; 1% err.)

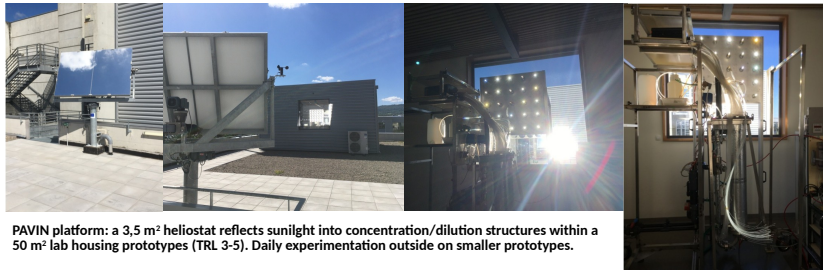
$C_x = 0.05 \text{ g/l}$	C1 (Rochatte)	C2 (Dauchet)	diff.	max
$\langle A \rangle (\mu\text{mol}/\text{s}/\text{m}^3)$	43550	18136	58%	46667
$\langle r_{O_2} \rangle (\text{mol}/\text{l}/\text{h})$	$4.39 \cdot 10^{-4}$	$4.25 \cdot 10^{-4}$	3%	$19 \cdot 10^{-4}$

$C_x = 0.10 \text{ g/l}$	C1 (Rochatte)	C2 (Dauchet)	diff.	max
$\langle A \rangle (\mu\text{mol}/\text{s}/\text{m}^3)$	46200	38100	18%	46667
$\langle r_{O_2} \rangle (\text{mol}/\text{l}/\text{h})$	$8.45 \cdot 10^{-4}$	$8.27 \cdot 10^{-4}$	1%	$19 \cdot 10^{-4}$

Conclusions & Perspectives

- Radiative properties are variable
 - illumination → pigment content
 - mixing → size and shape of the micro-organisms
- The grey approximation accuracy depends on radiative properties
 - cyanobacteria have "almost grey" spectral properties
 - use caution if spectral variations are sharp
 - eukaryotes (e.g. *chlamydomonas reinhardtii*)
 - photosensitizers for artificial photosynthesis (100% error)
- Simplification of the system geometry is not always possible
 - high energetic performance requires internal illumination (NPGC ESA project) leading to complex geometries
- Two-flux approximation, in our test case
 - can lead to 50% error on radiative transfer
 - but 2% error on $\langle r_{O_2} \rangle$ for cyanobacteria (no respiration)

Thank you for your attention



PAVIN platform: a 3,5 m² heliostat reflects sunlight into concentration/dilution structures within a 50 m² lab housing prototypes (TRL 3-5). Daily experimentation outside on smaller prototypes.